JUET Research Journal of Science & Technology
5 (2), July 2019, 01-07
http://www.publishingindia.com/juet

Experimental Investigation of Dimensional Accuracy During Micro-Machining of Inconel-718 Sheet

P. K. Shrivastava[1], B. Singh[2] and Y. Shrivastava[3*]

[1]Vidyavardhaka College of Engineering, Mysore, Karnataka, India.
[2]Jaypee University of Engineering and Technology, Guna, Madhya Pradesh, India.
[3]Galgotias College of Engineering and Technology, Greater Noida, Uttar Pradesh, India.
Email: yogeshshrivastava90@gmail.com
*Corresponding Author

Abstract: The traditional machining method is incapable of machine the Inconel-718 material due to its lower thermal properties, lower elastic properties and high chemical conductive at expanding temperature. The Nd: YAG laser cutting process provides better cutting quality, precision and geometric accuracy in shape or size. But due to high thermal properties, it is difficult to remove completely undesirable factors like the Top kerf width (TKW), Bottom kerf width (BKW) and kerf taper (KT). To improve the cutting quality of Inconel-718, experiments have been performed on a 300W pulsed Nd: YAG laser cutting system at various levels of input cutting parameters. Thereafter suitable artificial neural network has been adopted to develop mathematical models in terms of the aforementioned input cutting parameters for geometrical quality characteristics: Top Kerf Width, Bottom Kerf Width, and Kerf Taper. These developed models have been validated by comparing the predicted values with the experimental ones. Further, these models have been used to explore the dependency of input parameters on the responses and to predict a safe cutting range. At last, more experiments have been performed to validate the identified range. From the results, it has been found that the obtained optimal range of cutting parameters is significant.

Keywords: Artificial neural network, Dimensional accuracy, Inconel-718, Micro-machining.

I. Introduction

It is difficult to cut Inconel-718 using conventional machining techniques because of rapid work hardening during machining. Work hardening results in the plastic deformation of work-piece or tool. A large amount of cutting force is required to cut Inconel-718. This leads to high heat generation which results in the plastic deformation of the tool and thus deteriorating its life [1]. Conventional machining of Inconel-718 also results in inherent residual stresses which pose hindrances while surface finishing of final products as in aerospace structures [2]. Consequently, machining of this material using traditional methods is highly costly in comparison to the advanced machining techniques such as laser machining [3]. This motivated the researchers to adopt modern techniques of machining such as laser beam machining (LBM). Laser cutting is a very intricate and non-uniform process because of the involvement of different process parameters. The selection of appropriate laser and process parameters govern the quality, precision and geometrical accuracy of the cut [4, 5]. The selection of laser has been done on the basis of work reported by different researchers. They have examined that, Nd: YAG laser is suitable for machining of Al, Ti, Ni, and its alloys rather than the CO_2 laser. A laser beam with the pulsed mode is highly recommended for the cutting of high thermal conductive material because the pulsed laser beam delivers high peak power and minimizes the interaction time. However, high chemical affinity and low thermal conductivity of Ti, Ni and its alloys pose hindrances in achieving better cut qualities. Various researchers studied the cutting behavior of Ti, Ni and its alloys in different circumstances. The low-pressure oxygen gas is responsible for the uncontrolled burning and degraded surface. Shanjin and Yang [6] have used Nd: YAG laser for the cutting of 1 mm thick titanium alloy sheets. They also studied the effects of input process parameters on selected output quality characteristics: surface morphology, corrosion resistance, and heat-affected zone. When nitrogen and oxygen gas is used as an assist gas in laser cutting, it reacts with titanium and creates a fine layer of their nitrides and oxides. This is responsible for high HAZ.

Araujo *et al*. [7] reported that the CO_2 laser used for the cutting holes in aluminum alloys (Al 2024 T3) resulted in microstructure changes due to HAZ. Some researchers have also studied the effects of cutting parameters on the surface, geometric and thermal quality parameters during the Nd: YAG laser cutting of Inconel-718 sheet [8-10]. Moreover, few researchers have also investigated the effect of high power

CO_2 and Nd: YAG lasers on the Inconel-718 sheet [11, 12]. The kerf quality and metallurgical changes have also been examined using a profile projector and scanning electron microscopy during the laser cutting of Inconel-718 [13]. From the experimental investigation,they have found that the difficult to cut materials can be processed more suitably using Nd: YAG in pulsed mode.

In the past, a lot of works have been reported regarding this aspect of laser machining for various difficult to cut materials. They have adopted various techniques in order to explore the effect of the aforementioned parameters on the cut quality. Still many aspects of this domain are yet to be explored. Till date, very few methodologies have been suggested by the researchers regarding the development of a robust prediction model which can suggest the desired range of optimal process parameters for accomplishing the desired cut quality characteristics during cutting of Inconel-718 sheets. These factors motivated the present research work.

In the present work, experiments have been performed on pulsed Nd: YAG laser for the cutting of 1.4 mm thick Inconel-718 sheet. The input parameters considered are, gas pressure, standoff distance, cutting speed and laser power whereas top kerf width (TKW), bottom kerf width (BKW) and kerf taper (KT) have been selected as responses. The obtained experimental data have been further used to develop mathematical models considering three activation functions namely TANSIG, LOGSIG and PURELIN in the artificial neural network. The developed models have been explored to determine the dependency of responses on the input parameters. Further, a safe cutting range has been identified which is capable of minimizing the cutting defects. At last the obtained range has been validated by performing more experiments. From the results, it has been found that the obtained cutting range is significant.

II. Experimentation

In the present experimental study, the 300W (CNC-PCT 300) pulsed Nd: YAG laser cutting system connected with the CNC work table has been used for the conduction of experiments as shown in Fig. 1. Inconel-718 has been used as the work-piece material. Experiments have been performed on a 1.4 mm thick Inconel-718 sheet. The chemical composition of the Inconel-718 has been presented in Table I. Assist gas pressure, standoff distance, cutting speed and laser power have been selected as input process parameters or control factors for the laser cutting of Inconel- 718. The ranges and levels of process parameters considered have been shown in Table II. After the selection of cutting parameters and their respective levels, experiments have been conducted as shown in Table III.

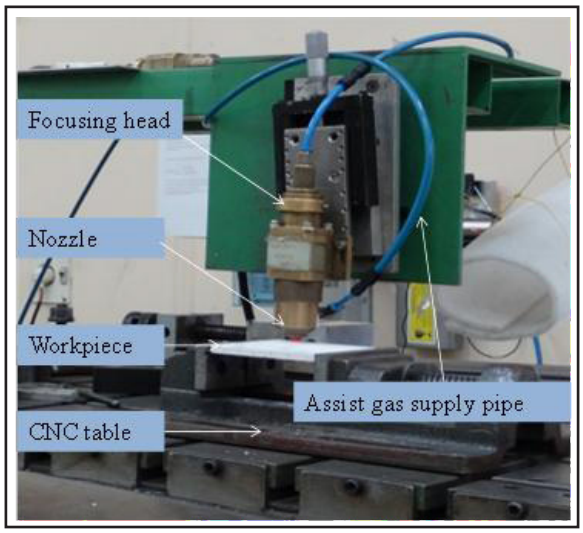

Fig. 1: Experimental Setup of Nd: YAG Laser

Table I: Chemical Composition of Inconel-718

Ni	Cr	Nb	Mo	Ti	Al	C	B	Si	Fe
53.60	18.20	5.06	3.04	0.97	0.44	0.052	0.003	0.10	Balance

Table II: Control Factors and their Levels Used for Laser Cutting of Inconel-718 Sheet

Symbol	Input Parameter	Unit	Level-1	Level-2	Level-3
A	Gas Pressure	(bar)	6	7	8
B	Standoff Distance	(mm)	0.5	1	1.5
C	Cutting Speed	(mm/min.)	20	30	40
D	Laser Power	(W)	220	240	260

In the present work, measured quality characteristics are top kerf width, bottom kerf width, and kerf taper. Stereo optical microscope with 160x magnification has been used for measuring these quality characteristics. The quality characteristics have been calculated using the following equations:

$$TKW = \left(\frac{K_1 + K_2 + K_3 + K_4}{4} \right) \quad (1)$$

$$BKW = \left(\frac{K_1' + K_2' + K_3' + K_4'}{4} \right) \quad (2)$$

$$KT = \left(\frac{TKW\text{-}BKW}{2t} \right) \times \frac{180}{\pi} \quad (3)$$

TABLE III: EXPERIMENTAL VALUES UN-CODED

Sr. No.	A	B	C	D	TKW	BKW	KT
1	7	0.5	30	240	0.693	0.433	4.726
2	6	0.5	30	260	0.709	0.521	3.870
3	6	1.5	30	220	0.692	0.466	4.665
4	6	1	30	260	0.717	0.502	4.287
5	8	0.5	30	260	0.696	0.499	4.751
6	7	1	30	260	0.703	0.477	4.855
7	8	0.5	40	220	0.693	0.501	4.297
8	6	0.5	40	260	0.734	0.518	4.363
9	7	1	40	240	0.719	0.455	5.275
10	7	1	30	240	0.713	0.494	4.821
11	6	1.5	40	240	0.756	0.506	4.249
12	8	1	20	260	0.711	0.449	5.293
13	7	1	20	240	0.695	0.437	4.651
14	8	1.5	20	220	0.705	0.495	4.797
15	8	1	40	240	0.765	0.468	5.564
16	6	0.5	40	240	0.697	0.489	4.255
17	8	1	20	220	0.737	0.504	4.564
18	7	1.5	40	220	0.786	0.630	3.918
19	7	1.5	30	220	0.774	0.483	5.303
20	6	0.5	40	220	0.697	0.477	4.883
21	6	1.5	30	240	0.687	0.502	4.355
22	7	0.5	20	260	0.788	0.601	5.108
23	6	0.5	20	240	0.741	0.558	4.269
24	6	0.5	20	220	0.710	0.504	4.606
25	8	0.5	20	260	0.694	0.423	4.461
26	8	0.5	20	240	0.696	0.468	4.585
27	6	1	40	260	0.709	0.480	4.815
28	6	1.5	40	220	0.752	0.520	4.212
29	7	1	20	260	0.701	0.466	4.578
30	8	1.5	40	240	0.692	0.456	4.729
31	6	1	40	240	0.743	0.517	3.900
32	7	1	30	220	0.762	0.524	4.625
33	8	1.5	30	220	0.700	0.473	4.497
34	6	1.5	20	260	0.697	0.460	4.660
35	6	1.5	20	240	0.704	0.448	5.289
36	7	0.5	30	220	0.780	0.592	4.211
37	6	1.5	20	220	0.724	0.501	4.073
38	8	1	40	260	0.777	0.515	4.941
39	8	0.5	20	220	0.753	0.541	4.286
40	7	1.5	40	240	0.740	0.525	4.149
41	7	1	40	220	0.704	0.458	4.171
42	8	1.5	30	240	0.698	0.442	4.565
43	8	1.5	20	240	0.727	0.534	4.397
44	8	1.5	40	220	0.699	0.503	4.228
45	6	1	30	220	0.696	0.469	4.443

III. Artificial Neural Network

Artificial neural network (ANN) is inspired by the human nervous system. In this technique, the architecture comprises a set of input and output layers [14-16]. The ANN architecture considered in the present analysis has been shown in Fig. 2. MATLAB software has been used to train the ANN architecture. LEARNGDM and TRAINLM learning functions have been used for learning and training purposes. TANSIG, LOGSIG, and PURELIN activation functions have been used to evaluate the function values at the intermediate and output neurons.

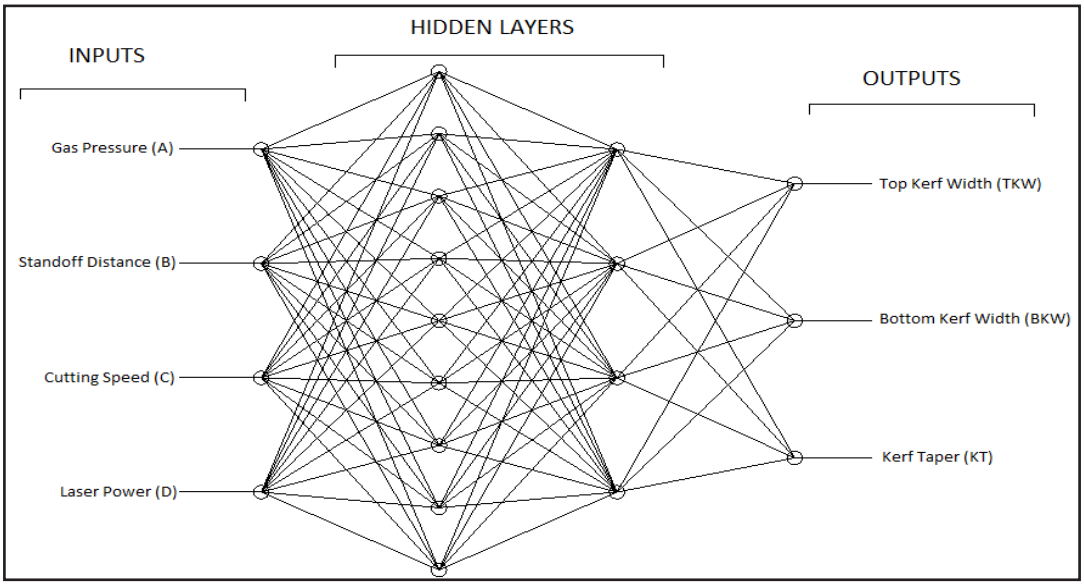

Fig. 2: ANN Architecture Used for the Analysis

In the present work, 45 experimental runs comprising of a random combination of the input parameters, have been considered for the training purpose. These 45 combinations of experimental runs have been shown in Table III. From Table III it is obvious that the magnitude of input parameters is not numerically comparable. For example, the range of laser power is 220-260 and that of standoff distance is 0.5-1.5. So, in order to avoid this variability and thus to maintain the uniformity among the input variables, all the variables have been normalized and presented in the coded form. In the present study, ANN training has been done considering the three activation functions viz. TANSIG, LOGSIG, and PURELIN. Prediction models of quality characteristics corresponding to these three activation functions have been developed. Predicted values using these models have been compared with the experimental ones. Finally, among these prediction models, the most accurate and suitable model has been selected on the basis of percentage deviation between the predicted and experimental values. The detailed analysis considering the aforementioned activation functions has been present in the ensuing section.

A. Comparison of Models Developed Using Three Transfer Functions

In the present section, the mathematical models developed for TKW, BKW, and KT have been compared. From the validation check of the models developed using TANSIG function, it has been found that % error in prediction has been found to be 1.762%, 1.335% and 7.221% for TKW, BKW, and KT, respectively. For LOGSIG function, the % error in prediction has been evaluated to be 4.901%, 4.599% and 12.749% for the TKW, BKW, and KT, respectively. Similarly, for PURELIN function, the % error has been found to be 7.497%, 6.853% and 14.254% for TKW, BKW, and KT, respectively. It has been inferred that among these ANN models, TANSIG function is the most accurate and suitable prediction model. Finally, on comparing cubic and TANSIG models, it is concluded that ANN TANSIG model is better one among all the models. Thereafter, the dependency of the responses on the input parameters has been explored for identifying a safe cutting range as discussed in the ensuing sections.

B. Parametric Effects

For determining the exact behavior of TKW, BKW and KT with respect to cutting parameters, 3D and contour plots have been drawn from the experimental results. The most influencing interaction parameters have been identified and their plots have been shown in Figs. 3-5.

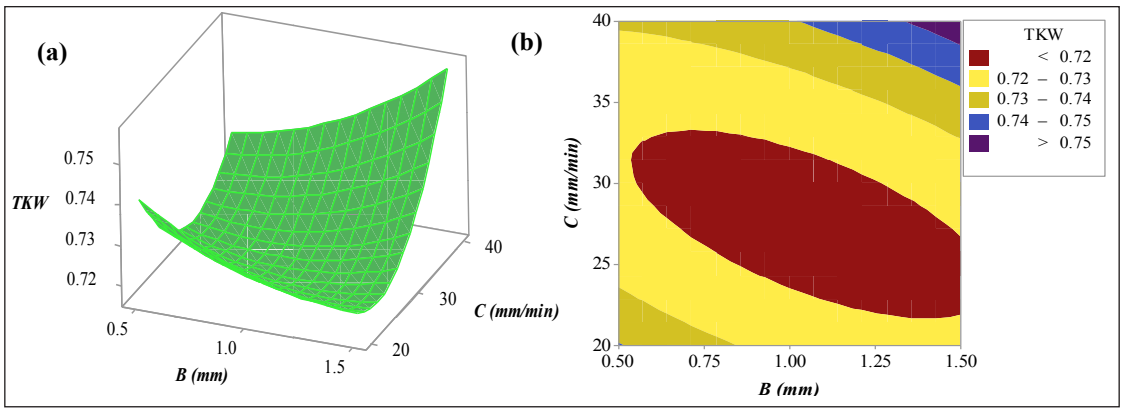

Fig. 3: Effect of Standoff Distance (B) and Cutting Speed (C) on TKW (a) Surface Plot and (b) Contour Plot

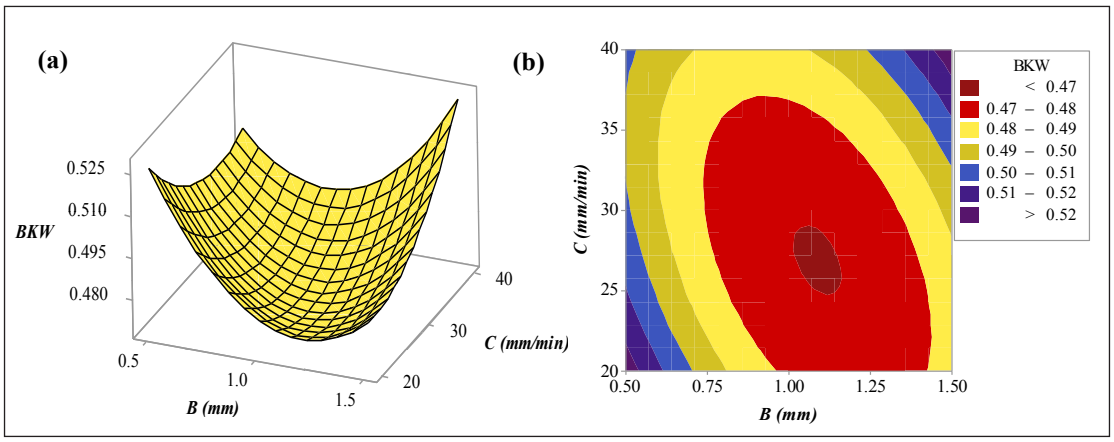

Fig. 4: Effect of Standoff Distance (B) and Cutting Speed (C) on BKW (a) Surface Plot and (b) Contour Plot

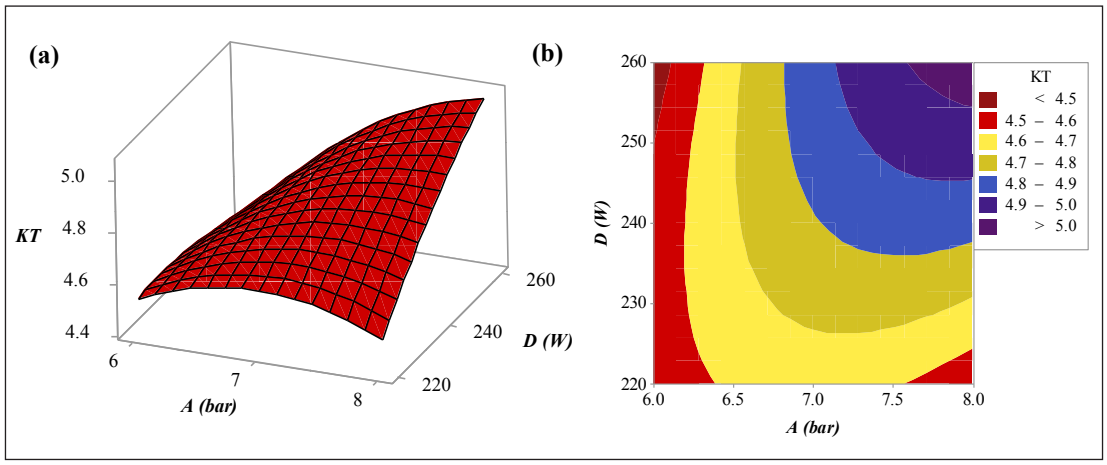

Fig. 5: Effect of Gas Pressure (A) and Pulse Frequency (D) on KT (a) Surface Plot and (b) Contour Plot

In these figures, the region with red color resembles the minimum value of responses. While the region with blue and purple color reflects the region with maximum value of responses. The region with the yellow color indicated the moderated value of responses. The effects of cutting speed and standoff distance has been shown in Fig. 3. From Fig. 3 it has been observed that at the initial level of standoff distance TKW is higher and on further increasing the value of standoff distance up to mid and higher level TKW starts to reduce. In case of cutting speed, initially, TKW is minimum and further on increasing the value of cutting speed up to higher-level TKW starts to increase gradually.

At the initial level of standoff distance, TKW is higher because at that moment gap between the workpiece and the laser beam is minimum due to which the laser beam does not penetrate properly and results in uneven heat distribution. Moreover, on increasing the value of standoff distance up to

mid and higher level, the distance between the laser beam and workpiece increases and hence the laser beam penetrates properly resulting in proper heat distribution. Similarly, at the initial level of cutting speed TKW is minimum because of this moment interaction time of laser beam and workpiece is high and the laser beam properly penetrates the workpiece. Due to this proper penetration heat distribution becomes even and the value of TKW has been noted minimum. Further on increasing the value of cutting speed up to mid and higher level TKW tends to increases because at this moment interaction time of laser beam and workpiece is less. Due to this lower interaction time, the laser beam does not penetrate properly resulting in un-even melting of the material and increasing trend of TKW.

Moreover, in the case of BKW, as shown in Fig. 4, at the initial level of standoff distance the gap between laser beam and workpiece is minimum due to which the laser beam is not penetrating properly and melted material is not ejected from the bottom surface appropriately. At this moment some amount of molten material stuck in the cutting surface and hence increases the BKW. Further, on increasing the value of standoff distance the gap between the laser beam and workpiece increases and now the laser beam is well focused, hence penetrating properly. This proper penetration results in even heat distribution from top to bottom.

Fig. 5 represents the surface and contour plot for kerf taper. These plots shows that, at the initial level of gas pressure the value of KT is minimum because, at that moment the value of laser power is also minimal due to which less amount of molten material is available and this molten material can be easily ejected by the available gas pressure from the bottom surface and hence the value of KT is minimum. On further increasing the value of laser power, a high amount of material is melting and the available gas pressure is not sufficient in ejecting the molten material properly. Hence some of the molten material re-solidifies within the cutting reason. Due to the solidification the value of KT increases.

C. Prediction of Safe Cutting Range

The interaction plots obtained from the experimental analysis has been further explored to identify a safe cutting range of input parameters at which the value of responses is minimum. For determining the safe cutting range the different interaction plots have been merged together and an interaction table has been constructed as shown in Table IV.

For acceptable values of TKW, the standoff distance should be kept between 0.55-1.50 mm with cutting speed between 22-33 mm/min as shown in Fig. 3. Similarly, for acceptable values of BKW, standoff distance should be kept between 0.8-1.4 mm with cutting speed between 20-36 mm/min as shown in Fig. 4. For acceptable values of KT, gas pressure should be kept between 7.5-8 bar with laser power between 220-230W.

Table IV: Safe Cutting Range

	TKW	BKW	KT	Safe Cutting Range
GAS PRESSURE (bar)			7.5-8	7.5-8
STANDOFF DISTANCE (mm)	0.55-1.50	0.8-1.4		0.8-1.4
CUTTING SPEED (mm/min.)	22-33	20-36		22-33
LASER POWER (W)			220-230	220-230

Moreover, the predicted safe cutting zone has been verified by performing more experiments. The set of experiments considered. From the results, it has been perceived that the obtained safe cutting zone is significant for the given set of input parameters and levels.

Table V: Confirmatory Experiments

Sr. No.	A	B	C	D	TKW	BKW	KT
1.	7.5	0.8	30	220	0.729	0.487	4.561
2.	8	1	30	230	0.731	0.471	4.595
3.	8	1.4	30	230	0.727	0.474	4.683

IV. Conclusion

In the present work, experiments have been performed and mathematical models for TKW, BKW, and KT have been developed by using three transfer functions TANSIG, LOGSIG, and PURELIN. From the validation check of the models developed using TANSIG function, it has been found that % error in prediction has been found to be 1.762%, 1.335% and 7.221% for TKW, BKW, and KT, respectively. For LOGSIG function, the % error in prediction has been evaluated to be 4.901%, 4.599% and 12.749% for the TKW, BKW, and KT, respectively. Similarly, for PURELIN function, the % error has been found to be 7.497%, 6.853% and 14.254% for TKW, BKW, and KT, respectively. It has been inferred that among

these ANN models, TANSIG function is the most accurate and suitable prediction model. Finally, the dependence of response on the input parameters have been investigated and a safe cutting range has been determined. The obtained range has been validated by performing more experiments. From the results, it has been found that the obtained range is significant and it has been concluded that the proposed methodology seems helpful for ascertaining the optimal range of cutting parameters pertaining to good quality cut with appreciably higher precision and accuracy.

References

[1] K. Venkatesan, R. Ramanujam, and P. Kuppan, "Parametric modeling and optimization of laser scanning parameters during laser assisted machining of Inconel 718," *Optics & Laser Technology,* vol. 78, pp. 10-18, 2016.

[2] J. Zhou, J. Ren, and C. Yao, "Multi-objective optimization of multi-axis ball-end milling Inconel 718 via grey relational analysis coupled with RBF neural network and PSO algorithm," *Measurement,* vol. 102, pp. 271-285, 2017.

[3] K. Venkatesan, and R. Ramanujam, "Statistical approach for optimization of influencing parameters in laser assisted machining (LAM) of Inconel alloy," *Measurement,* vol. 89, pp. 97-108, 2016.

[4] A. K. Dubey, and V. Yadava, "Laser beam machining-A review," *International Journal of Machine Tools and Manufacture,* vol. 48, no. 6, pp. 609-628, 2008.

[5] A. Sharma, and V. Yadava, "Experimental analysis of Nd-YAG laser cutting of sheet materials – A review," *Optics & Laser Technology,* vol. 98, pp. 264-280, 2018.

[6] L. Shanjin, and W. Yang, "An investigation of pulsed laser cutting of titanium alloy sheet," *Optics and Lasers in Engineering,* vol. 44, no. 10, pp. 1067-1077, 2006.

[7] D. Araujo, F. Carpio, D. Mendez, A. Garcıa, M. Villar, R. Garcıa, D. Jimenez, and L. Rubio, "Microstructural study of CO2 laser machined heat affected zone of 2024 aluminum alloy," *Applied Surface Science,* vol. 208, pp. 210-217, 2003.

[8] D. Ahn, K. Byun, and M. Kang, "Thermal characteristics in the cutting of Inconel 718 superalloy using CW Nd: YAG laser," *Journal of Materials Science & Technology,* vol. 26, no. 4, pp. 362-366, 2010.

[9] A. Dong-Gyu, and B. Kyung-Won, "Influence of cutting parameters on surface characteristics of cut section in cutting of Inconel 718 sheet using CW Nd: YAG laser," *Transactions of Nonferrous Metals Society of China,* vol. 19, no. 1, pp. s32-s39, 2009.

[10] A. K. Dubey, and V. Yadava, "Multi-objective optimization of Nd: YAG laser cutting of nickel-based superalloy sheet using orthogonal array with principal component analysis," *Optics and Lasers in Engineering,* vol. 46, no. 2, pp. 124-132, 2008.

[11] D.-G. Ahn, and K.-W. Byun, "Investigation of cutting characteristics in the sharp comer for the case of cutting of inconel 718 super-alloy sheet using high-power CW Nd: YAG laser," *Journal of Welding and Joining*, vol. 26, no. 5, pp. 90-96, 2008.

[12] A. Hasçalık, and M. Ay, "CO_2 laser cut quality of Inconel 718 nickel–based superalloy," *Optics & Laser Technology,* vol. 48, pp. 554-564, 2013.

[13] K. Nyon, C. Nyeoh, M. Mokhtar, and R. Abdul-Rahman, "Finite element analysis of laser inert gas cutting on Inconel 718," *The International Journal of Advanced Manufacturing Technology,* vol. 60, pp. 995-1007, 2012.

[14] Y. Shrivastava, and B. Singh, "Possible way to diminish the effect of chatter in CNC turning based on EMD and ANN approaches," *Arabian Journal for Science and Engineering*, vol. 43, no. 9, pp. 4571-4591, November 2017.

[15] Y. Shrivastava, and B. Singh, "Stable cutting zone prediction in computer numerical control turning based on empirical mode decomposition and artificial neural network approach," *Transactions of the Institute of Measurement and Control*, vol. 41, no. 1, pp. 193-209, 2019.

[16] Y. Shrivastava, and B. Singh, "Stable cutting zone prediction in CNC turning using adaptive signal processing technique merged with artificial neural network and multi-objective genetic algorithm," *European Journal of Mechanics-A/Solids*, vol. 70, pp. 238-248, 2018.